

Supporting Information

Selective Separation of 2,5-Dimethylfuran and 2,5-Dimethyltetrahydrofuran using Nonporous Adaptive Crystals of a Hybrid[3]arene

Yang, Liu ^{1,2,†}, and Yitao Wu ^{1,2,†,*}

¹Stoddart Institute of Molecular Science, Department of Chemistry, Zhejiang University, Hangzhou 310058, P. R. China.

²ZJU-Hangzhou Global Scientific and Technological Innovation Center-Hangzhou Zhijiang Silicone Chemicals Co., LTD Joint Lab, Zhejiang-Israel Joint Laboratory of Self-Assembling Functional Materials, ZJU-Hangzhou Global Scientific and Technological Innovation Center, Zhejiang University, Hangzhou 311215, P. R. China.

[†]Yang Liu and Yitao Wu contribute equally to this work.

Corresponding author: yitaowu@zju.edu.cn.

Table of Content (26 pages)

1. Materials	S2
2. Methods	S2
3. Characterization of Activated Hybrid[3]arene	S3
4. Solid–Vapor Adsorption Experiments of Hybrid[3]arene	S7
5. Recycling Experiments of Hybrid[3]arene	S20
6. References	S25

1. Materials

All starting materials including 2,5-dimethylfuran (**DMeF**) and 2,5-dimethyltetrahydrofuran (**DMeTHF**) were purchased commercially and used as received. Hybrid[3]arene (**HB3**) was synthesized as described previously.^{S1} Activated crystalline **HB3** was denoted as **HB3 α** . **HB3 α** was prepared according to the previous report.^{S2} All the mixture in this work were $v:v = 1:1$ unless specifically noted.

Table S1 Physical properties of **DMeF** and **DMeTHF**.^{S3}

Substance	Melting point (°C)	Boiling point (°C)	Saturated vapor pressure at 298 K (kPa)
DMeF	-62.8	96.0	57.1 \pm 0.2 mmHg
DMeTHF	-62.8	91.0	62.1 \pm 0.1 mmHg

2. Methods

2.1. Powder X-Ray Diffraction (PXRD)

The PXRD data were collected on a Rigaku Ultimate-IV X-Ray diffractometer operating at 40 kV/30 mA using the Cu K α line ($\lambda = 1.5418$ Å). Data were measured over the range 5–35° in 5°/min steps over 8 min.

2.2. Thermogravimetric Analysis (TGA)

TGA analysis was carried out using a Q5000IR analyzer (TA Instruments) with an automated vertical overhead thermobalance. The samples were heated at 10 °C/min using N₂ as the protective gas.

2.3. Single Crystal Growth

Single crystals of **DMeF@HB3** were grown by placing 5.00 mg of dry **HB3** powder in a small vial, adding 1 mL of **DMeF**, heating until all the powder was dissolved, and allowing to evaporate at room temperature about one week.

2.4. Single Crystal X-ray Diffraction (SCXRD) Analyses

Single crystal X-ray diffraction data were collected on a Bruker D8 VENTURE CMOS X-ray diffractometer with a graphite monochromated Mo-K α radiation ($\lambda = 0.71073$ Å).

2.5. Solution ¹H NMR Spectroscopy

Proton nuclear magnetic resonance (¹H NMR) spectra were recorded using a Bruker Avance III DMX 400 spectrometer, a Bruker Avance III DMX 500 spectrometer, and an Agilent DD2-600 spectrometer.

2.6. Gas Chromatography (GC)

Gas chromatography analysis: GC measurements were carried out using an Agilent 7890B instrument configured with a FID detector and a DB-624 column (30 m × 0.53 mm × 3.0 μm). Samples were analyzed using headspace injections and were performed by incubating the sample at 120 °C for 30 min followed by sampling 1.00 mL of the headspace. The following GC method was used: the oven was programmed from 50 °C, and ramped in 10 °C min⁻¹ increments to 150 °C with 15 min hold; the total run time was 25 min; the injection temperature was 250 °C; the detector temperature was 280 °C with nitrogen, air, and make-up flow-rates of 35, 350, and 35 mL min⁻¹, respectively; helium (carrier gas) flow-rate was 3.0 mL min⁻¹. The samples were injected in the split mode (30:1).

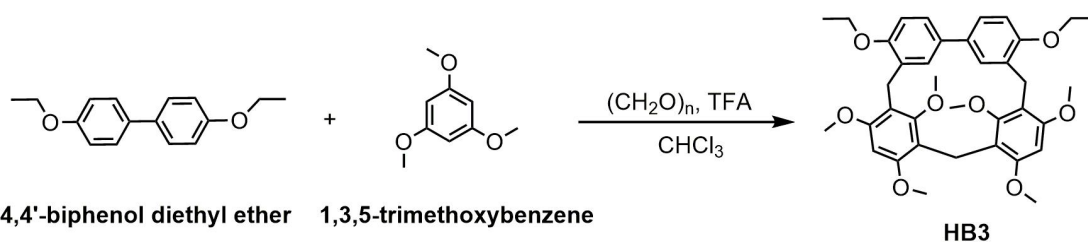
2.7. Gas sorption measurements

N₂ adsorption and desorption isotherms for the activated materials were measured at 77 K using a JW-BK200C 2 instrument.

2.8. Theoretical calculations

The geometry optimization and density functional theory (DFT) chemical description for the molecular structures of all **DMeF** and **DMeTHF** compounds were performed using Gaussian09 program^{S4} package with M062X exchange-correlation functional and 6-311G** basis set^{S5-S6}.

3. Characterization of Activated Hybrid[3]arene



Scheme S1. Synthetic route to hybrid[3]arene (**HB3**)

Synthesis of **HB3**: To the solution of 4,4'-biphenol diethyl ether (2.42 g, 10.0 mmol) and 1,3,5-trimethoxybenzene (3.36 g, 20.0 mmol) in CHCl₃ (200 mL), paraformaldehyde (0.900 g, 30.0 mmol) and trifluoroacetic acid (TFA, 10 mL) were added. The mixture was refluxed for 30 min, and the progress was monitored by thin-layer chromatography (TLC). The mixture was cooled to room temperature, and an excess of saturated aqueous Na₂CO₃ was added to neutralize TFA. The organic phase was separated and the crude product was purified by column chromatography (petroleum ether/ CH₂Cl₂, v/v 10:1 to 3:1) to get **HB3** as a white solid (1.67 g, 25%).

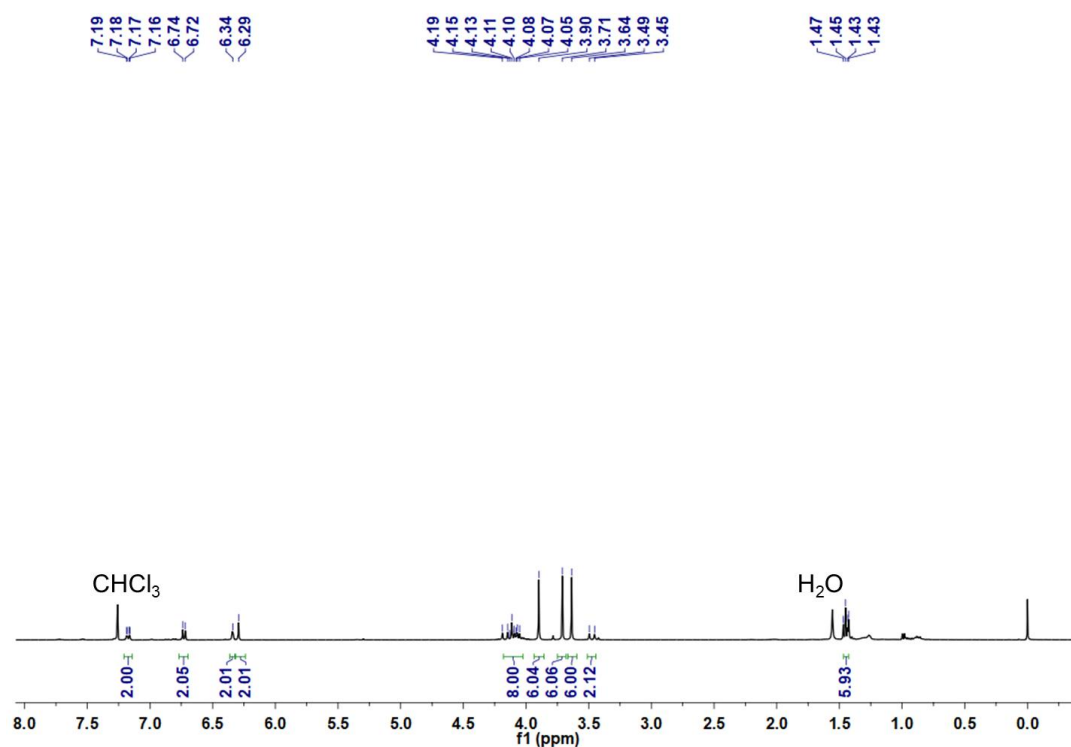


Fig. S1. ¹H NMR spectrum (600 MHz, chloroform-*d*, 298 K) of **HB3**.

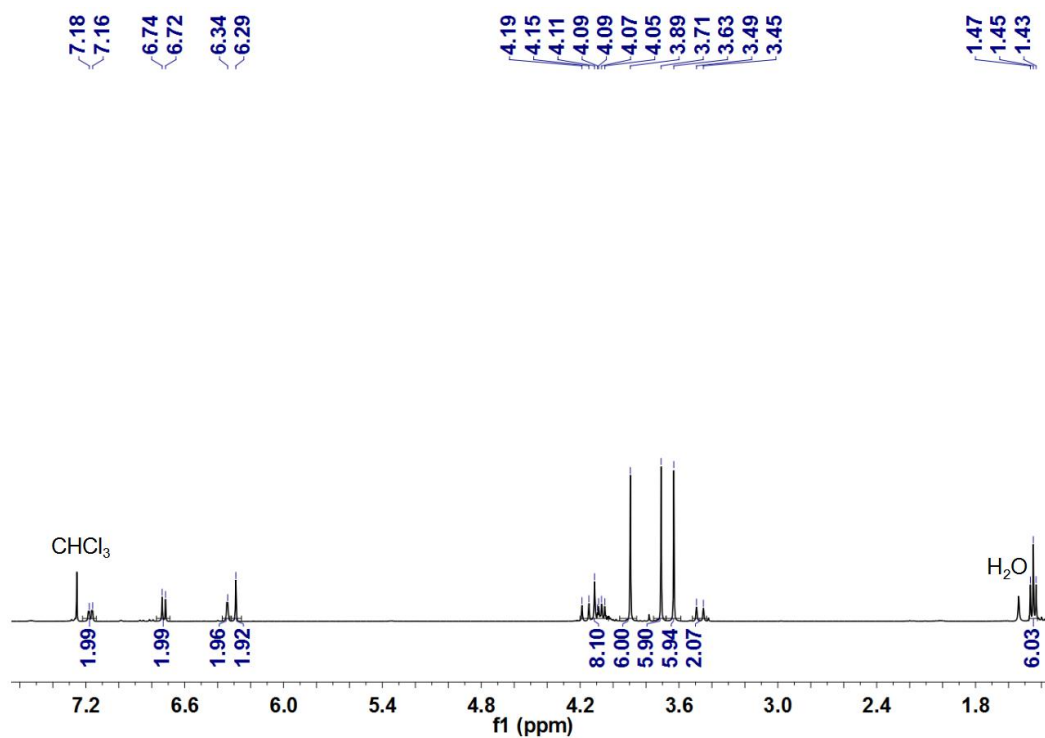


Fig. S2. ¹H NMR spectrum (600 MHz, chloroform-*d*, 298 K) of **HB3α**.

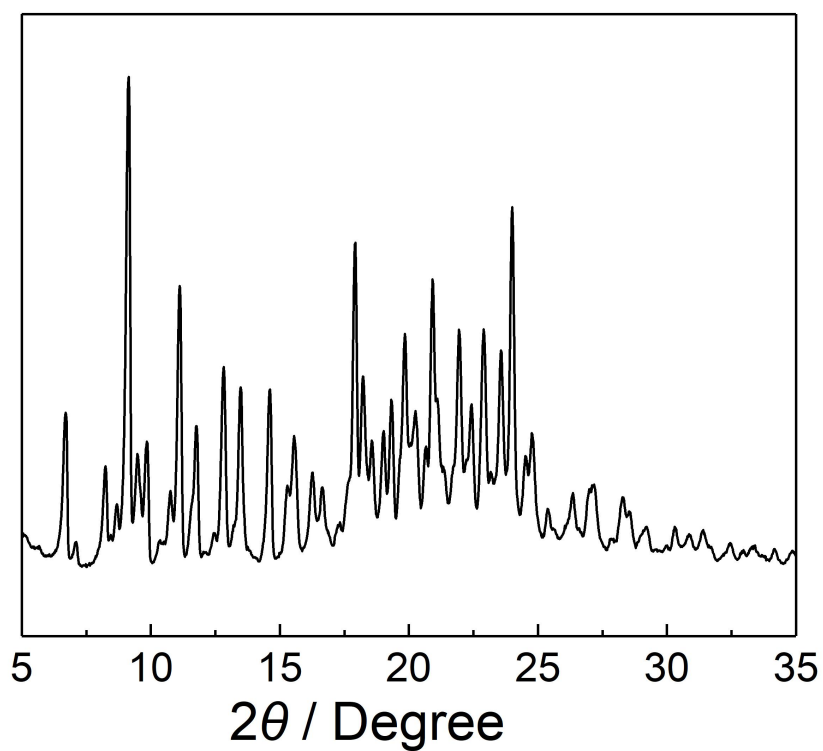


Fig. S3. PXRD pattern of **HB3α**.

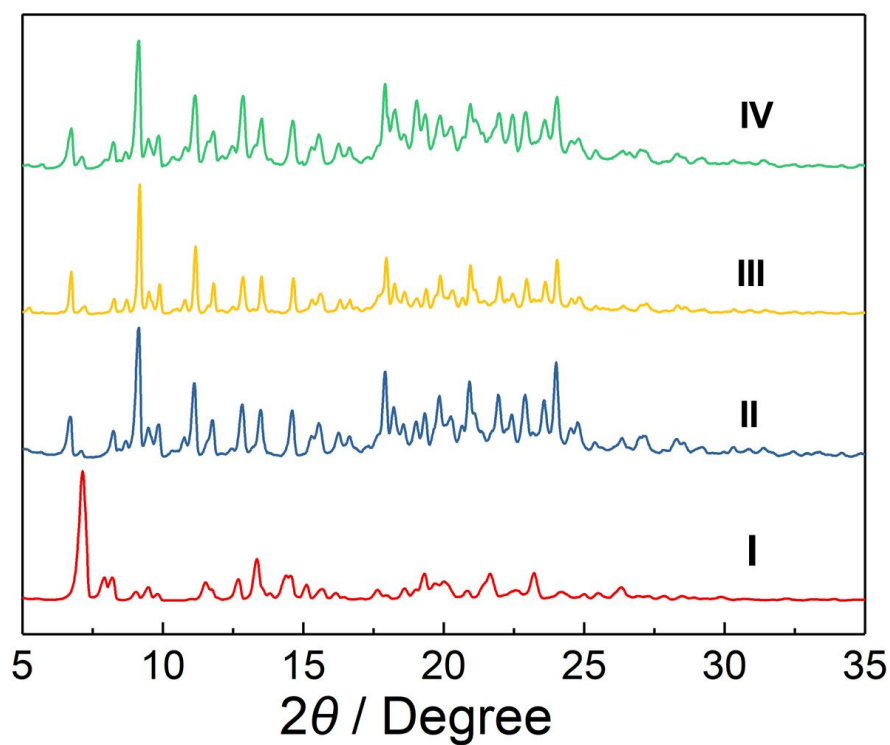


Fig. S4. PXRD patterns of (I) as-synthesized **HB3**; (II) **HB3** under vacuum; (III) high temperature; (IV) humid environment conditions.

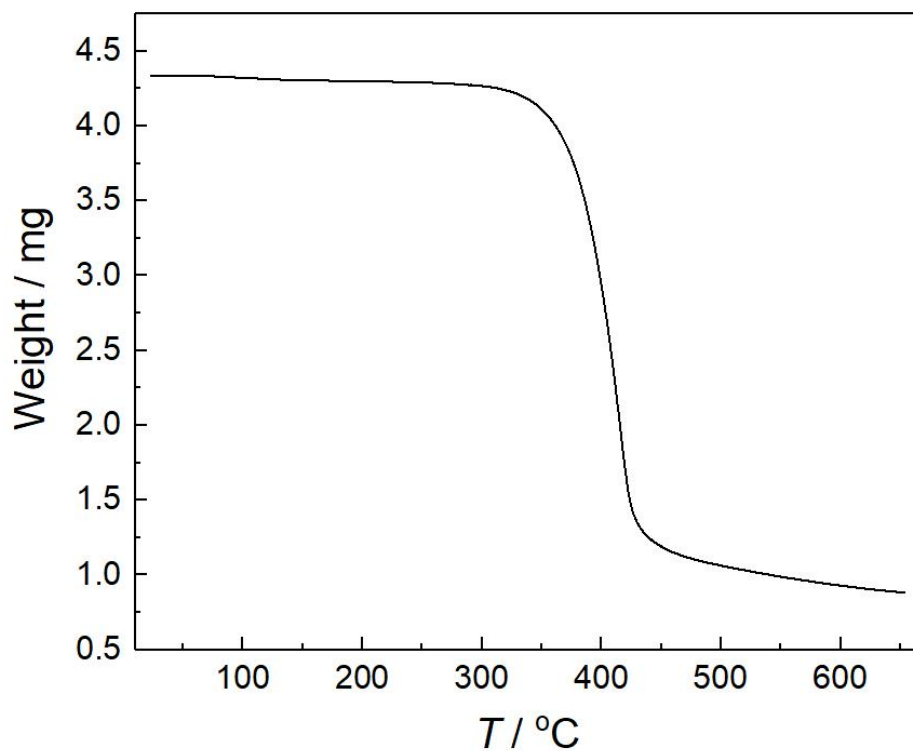


Fig. S5. TGA curve of desolvated **HB3 α** .

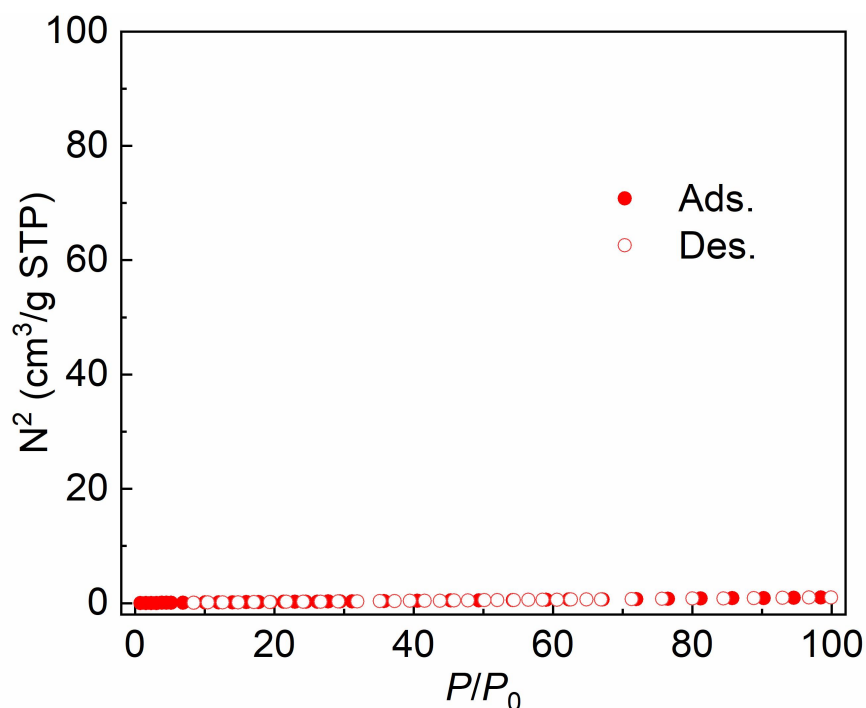


Fig. S6. Experimental N_2 adsorption isotherms at 77 K measuring the porosity of activated **HB3 α** . The apparent Brunauer-Emmett-Teller (BET) surface area is calculated to be $2 \text{ m}^2/\text{g}$, indicating **HB3 α** is nonporous.

4. Solid-Vapor Adsorption Experiments of Hybrid[3]arene

4.1. Single-Component DMeF and DMeTHF Adsorption Experiments

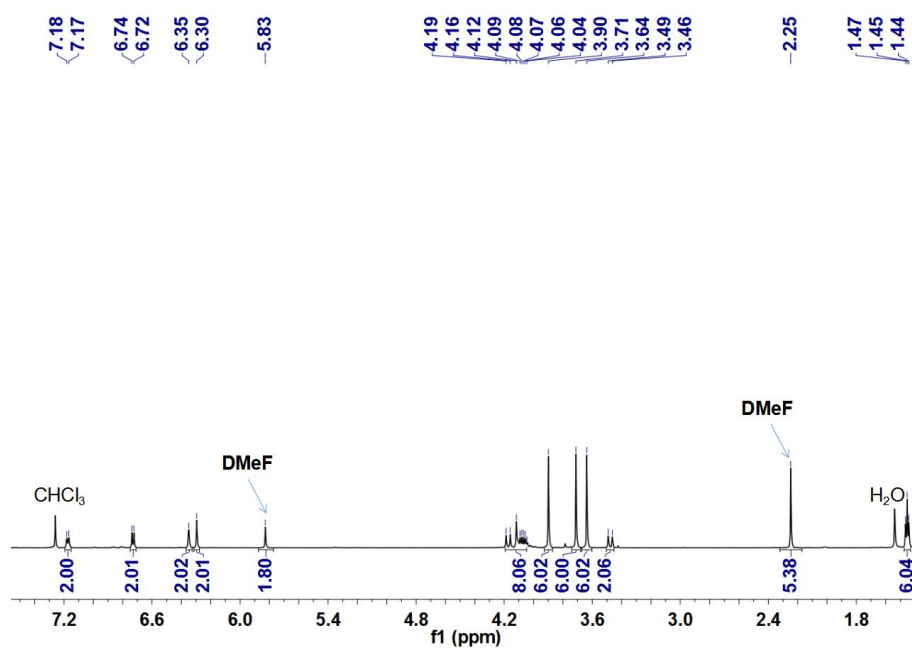


Fig. S7. ^1H NMR spectrum (600 MHz, chloroform-*d*, 298 K) of **HB3 α** after adsorption of **DMeF** vapor.

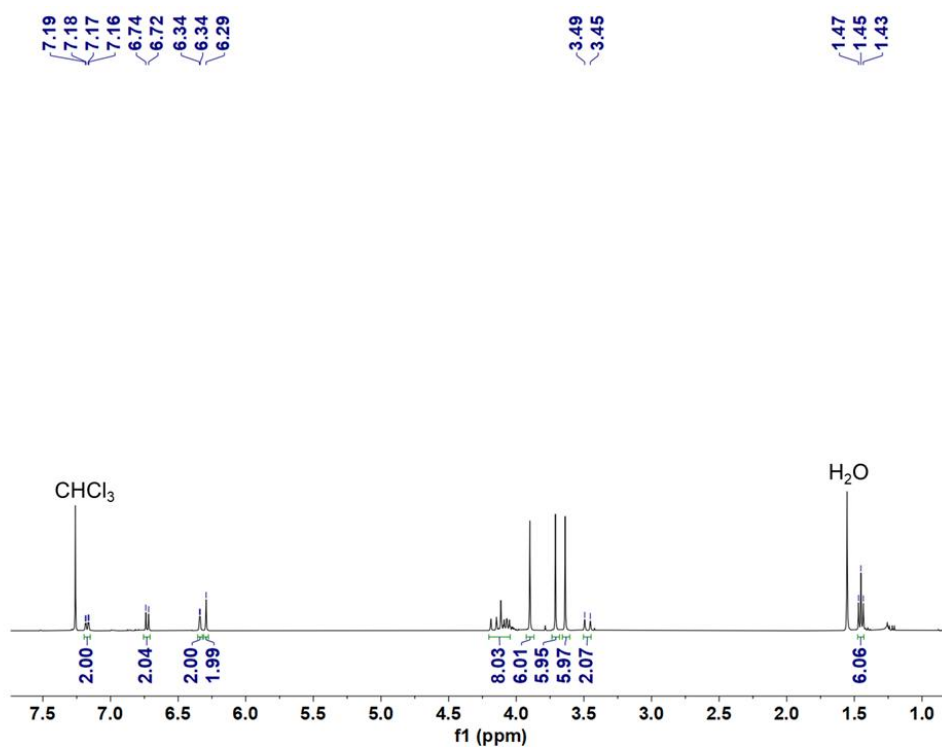


Fig. S8. ^1H NMR spectrum (600 MHz, chloroform-*d*, 298 K) of **HB3 α** after adsorption of **DMeTHF** vapor.

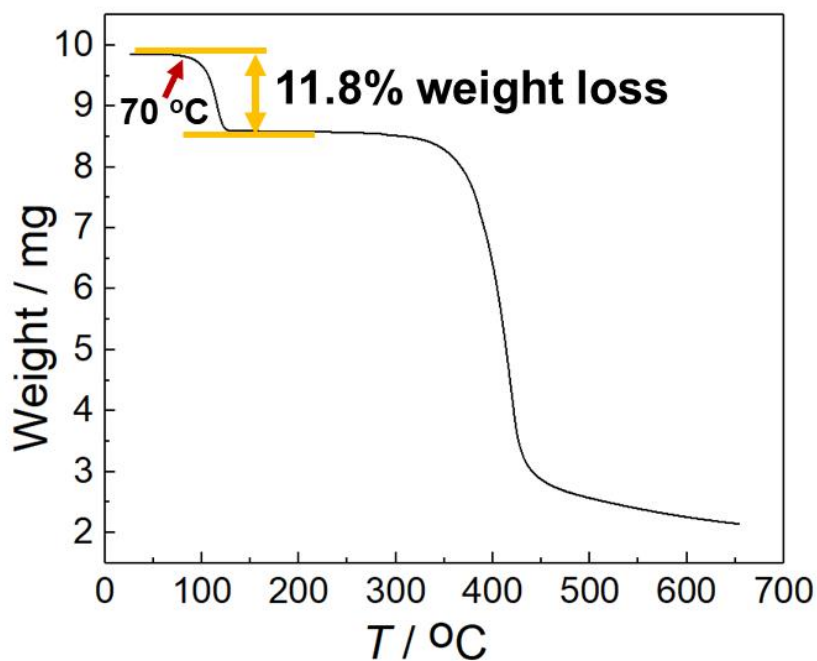


Fig. S9. TGA curve of desolvated **HB3 α** after adsorption of **DMeF** vapor. The weight loss below 150 °C can be calculated to one equivalent of **DMeF** molecule *per* **HB3** molecule.

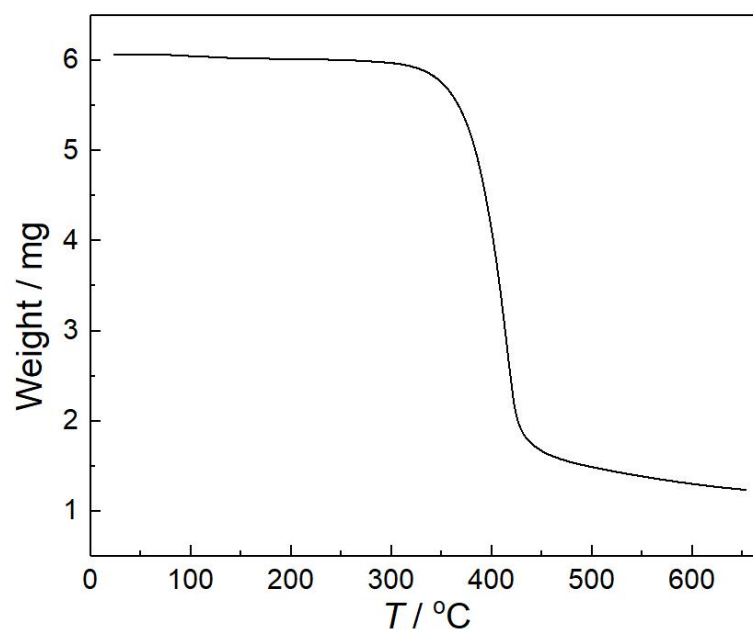


Fig. S10. TGA curve of desolvated **HB3 α** after adsorption of **DMeTHF** vapor. TGA results revealed no weight loss, indicating no uptake of **DMeTHF** vapor.

4.2. Structural Analyses of Single-Component Vapor Adsorption Experiments

Table S2. Experimental single crystal X-ray diffraction data of **DMeF@HB3** structure.

Formula	DMeF@HB3
Empirical formula	C ₄₃ H ₅₀ O ₉
Formula weight	710.83
Temperature/K	169.99
Crystal system	triclinic
Space group	<i>P</i> $\bar{1}$
<i>a</i> /Å	10.8040(3)
<i>b</i> /Å	13.0735(3)
<i>c</i> /Å	15.6468(4)
α /°	109.2350(10)
β /°	97.967(2)
γ /°	107.3160(10)
Volume/Å ³	1922.21(9)
<i>Z</i>	2
ρ_{calc} (g/cm ³)	1.228
μ /mm ⁻¹	0.443
<i>F</i> (000)	760
Crystal size/mm ³	0.13 × 0.12 × 0.1
Radiation	GaK α (λ = 1.34139)
2 θ range for data collection/°	6.754 to 109.886
Index ranges	-13 ≤ <i>h</i> ≤ 13, -14 ≤ <i>k</i> ≤ 15, -19 ≤ <i>l</i> ≤ 19
Reflections collected	19307
Independent reflections	7275 [<i>R</i> _{int} = 0.0894, <i>R</i> _{sigma} = 0.0986]
Data/restraints/parameters	7275/210/546
Goodness-of-fit on <i>F</i> ²	1.018
Final <i>R</i> indexes [<i>I</i> ≥ 2 σ (<i>I</i>)]	<i>R</i> ₁ = 0.0807, <i>wR</i> ₂ = 0.2057
Final <i>R</i> indexes [all data]	<i>R</i> ₁ = 0.1151, <i>wR</i> ₂ = 2377
Largest difference peak/hole/e Å ⁻³	0.35/-0.41
CCDC-number	1975518

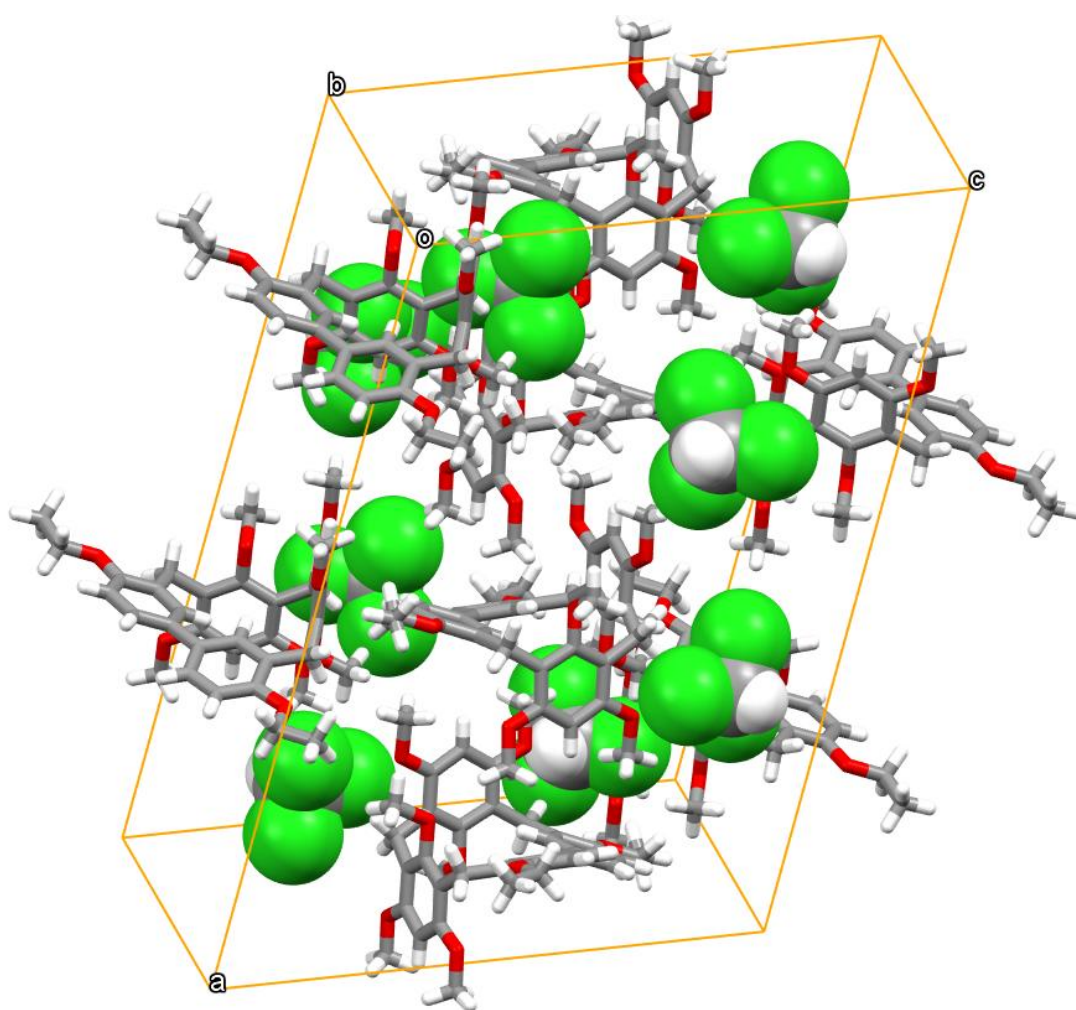


Fig. S11. Capped-stick and spacefill representation of the single crystal structure of $\text{CHCl}_3@HB3$ in a unit cell. The elementary cell is marked with an orange cuboid ($a = 28.16(6) \text{ \AA}$, $b = 14.15(3) \text{ \AA}$, $c = 19.61(4) \text{ \AA}$, $\alpha = 90^\circ$, $\beta = 106.28(10)^\circ$, $\gamma = 90^\circ$, space group: $C2/C$). Carbon atoms are grey, oxygen atoms are red, chlorine atoms are green, and hydrogen atoms are white.

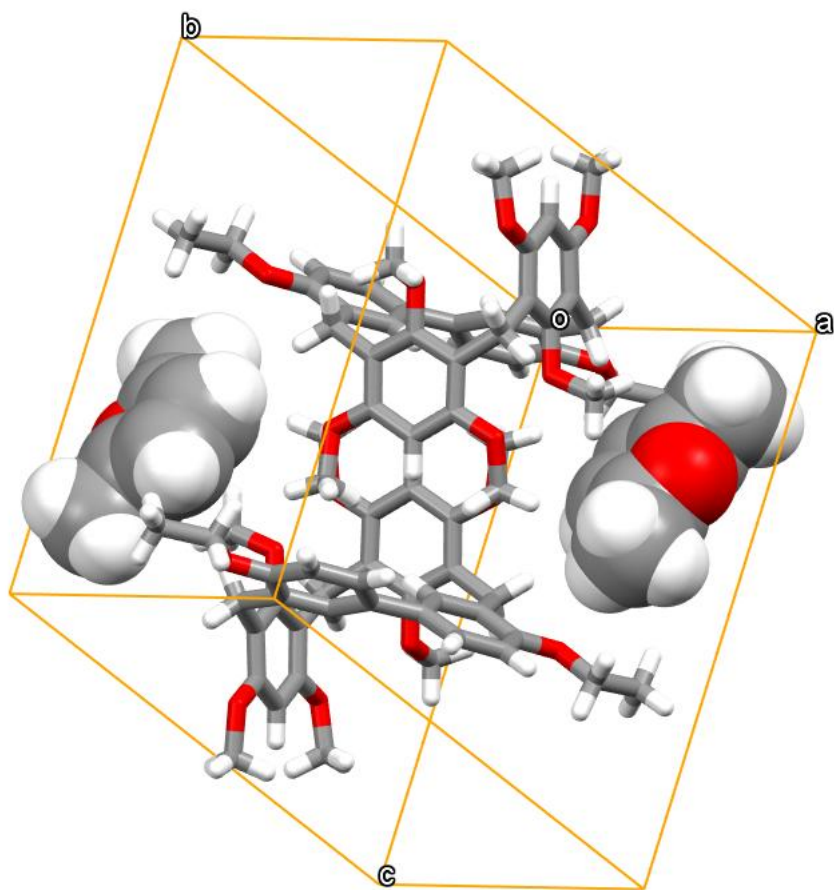


Fig. S12. Capped-stick and spacefill representation of the single crystal structure of **DMeF@HB3** in a unit cell. Carbon atoms are grey, oxygen atoms are red, and hydrogen atoms are white. The elementary cell is marked with an orange cuboid ($a = 10.80(3) \text{ \AA}$, $b = 13.07(3) \text{ \AA}$, $c = 15.65(4) \text{ \AA}$, $\alpha = 109.24(10)^\circ$, $\beta = 97.98(2)^\circ$, $\gamma = 107.32(10)^\circ$, space group: $P\bar{1}$). Compared with the single crystal structure of **CHCl₃@HB3**, the unit cell parameters have obvious difference, this also indicates the adaptive nature of **HB3** crystals.

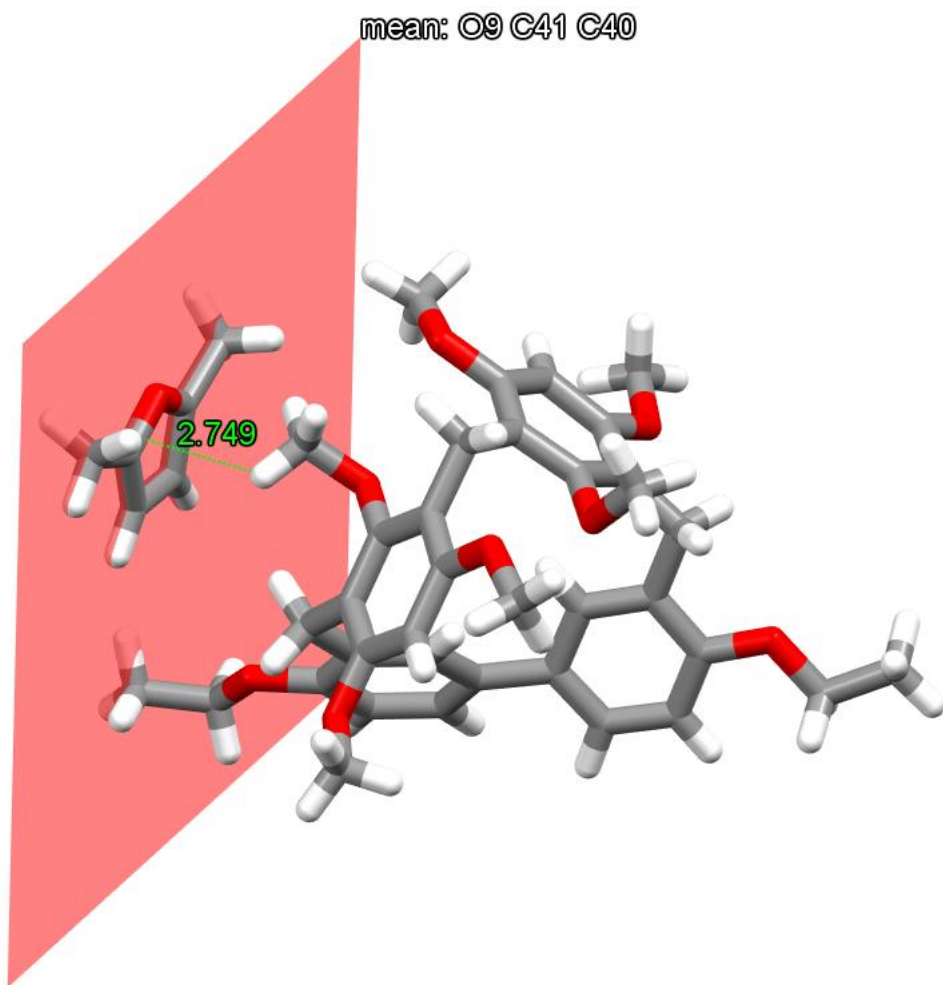


Fig. S13. Capped-stick representation of the single crystal structure of **DMeF@HB3**. Carbon atoms are grey, hydrogen atoms are white, and oxygen atoms are red. [C–H \cdots π] distance (Å) and angle (deg): 2.75, 134.34.

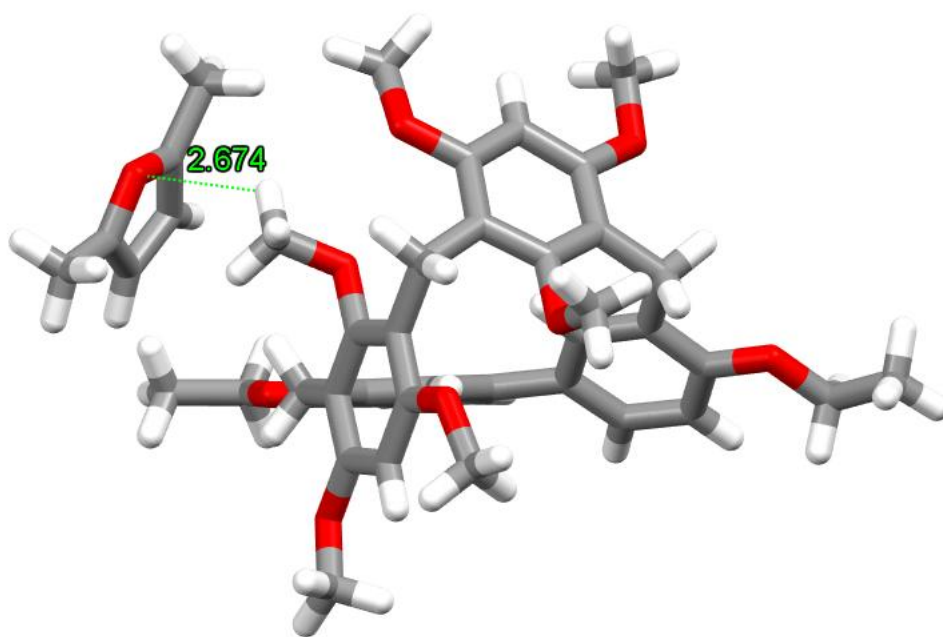


Fig. S14. Capped-stick representation of the single crystal structure of **DMeF@HB3**. Carbon atoms are grey, hydrogen atoms are white, and oxygen atoms are red. Hydrogen-bond parameters: [C...O] distances (Å), [H...O] distances (Å) and [C-H...O] angles (deg) of [C-H...O] hydrogen bonds, 3.22, 2.67, 115.17.

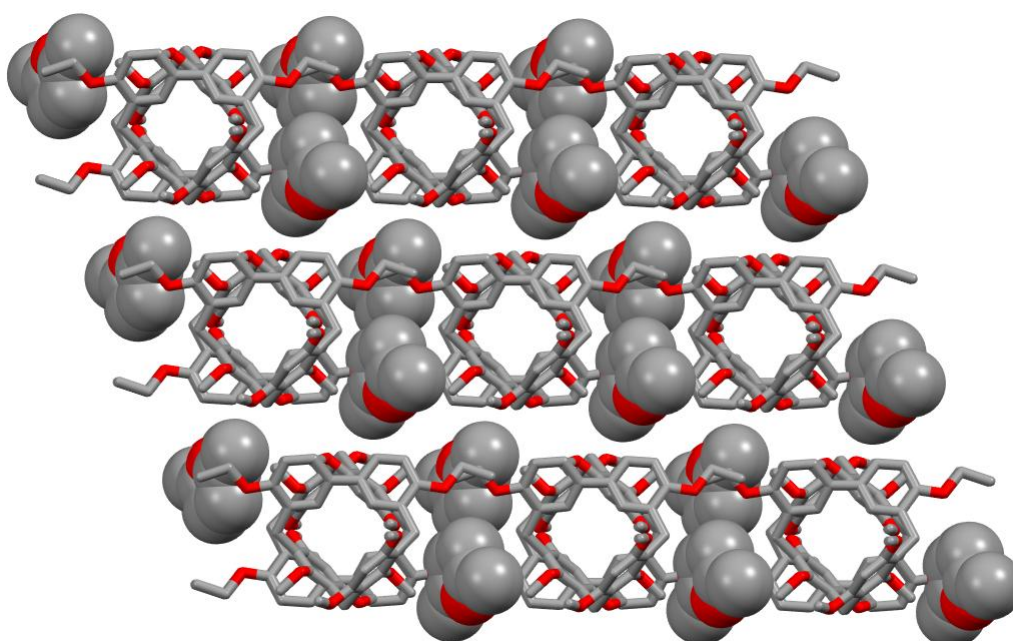


Fig. S15. Capped-stick and spacefill representation of the single crystal structure of **DMeF@HB3** in a packing mode. Carbon atoms are grey and oxygen atoms are red. Hydrogen atoms are omitted for clarity.

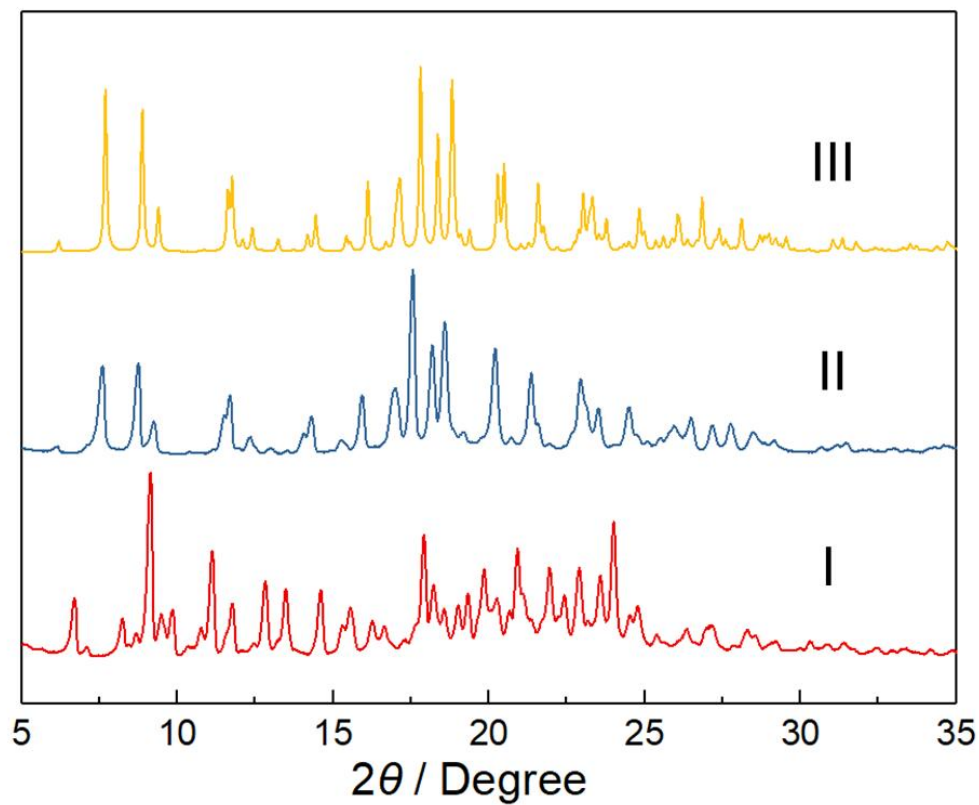


Fig. S16. PXRD patterns of **HB3**: (I) activated **HB3 α** ; (II) after adsorption of **DMeF** vapor; (III) simulated from single crystal structure of **DMeF@HB3**.

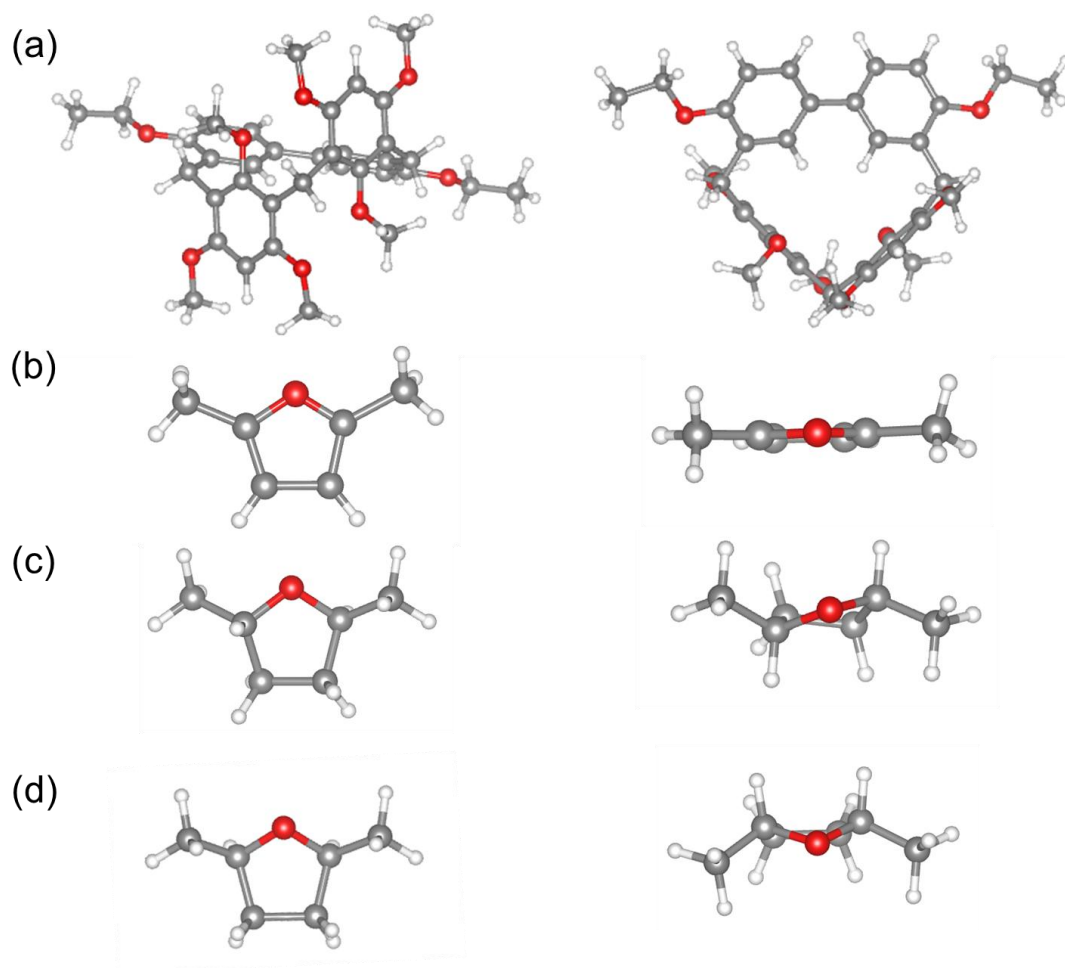


Fig. S17. The optimized structures of (a) **HB3**, (b) **DMeF**, (c) *trans*-**DMeTHF** and (d) *cis*-**DMeTHF**.

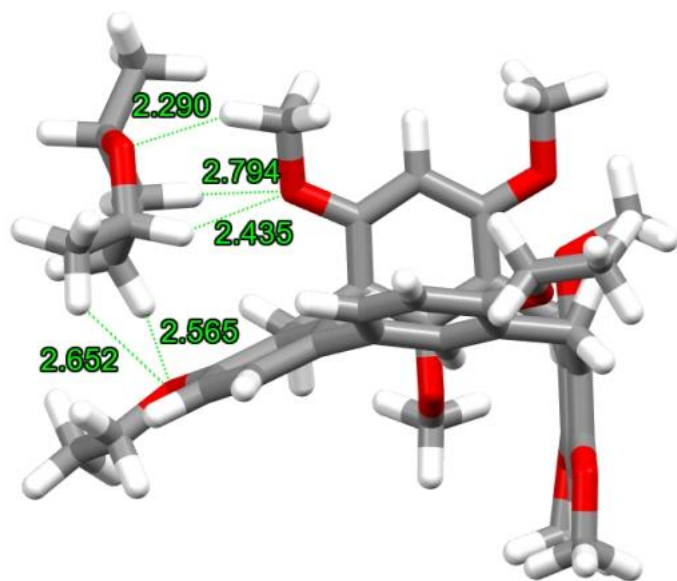


Fig. S18. Capped-stick representation of the calculated structure of *trans*-DMeTHF@HB3. Carbon atoms are grey, hydrogen atoms are white, and oxygen atoms are red. Hydrogen-bond parameters: [C...O] distances (Å), [H...O] distances (Å) and [C-H...O] angles (deg) of [C-H...O] hydrogen bonds, 3.25, 2.29, 145.60; 3.61, 2.79, 131.33; 3.29, 2.44, 133.07; 3.33, 2.57, 126.63; 3.46, 2.65, 130.09.

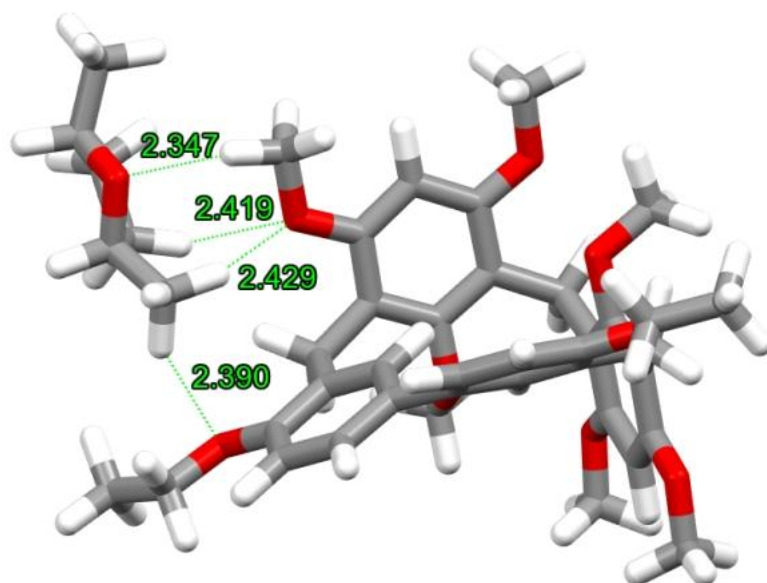


Fig. S19. Capped-stick representation of the calculated structure of *cis*-DMeTHF@HB3. Carbon atoms are grey, hydrogen atoms are white, and oxygen atoms are red. Hydrogen-bond parameters: [C \cdots O] distances (Å), [H \cdots O] distances (Å) and [C–H \cdots O] angles (deg) of [C–H \cdots O] hydrogen bonds, 3.42, 2.35, 166.01; 3.38, 2.42, 145.22; 3.39, 2.43, 145.83; 3.36, 2.39, 147.49.

Table S3. Calculated binding energies of DMeF/DMeTHF in HB3.

Substance	Number of guest molecules in HB3	E_{BE} (kJ/mol)
DMeF	1	–33.98
<i>trans</i> -DMeTHF	1	–30.75
<i>cis</i> -DMeTHF	1	–28.24

4.3. DMeF and DMeTHF Mixture Adsorption Experiments

For each mixture solid–vapor experiment, an open 5.00 mL vial containing 20.00 mg of guest-free HB3 α adsorbent was placed in a sealed 20.00 mL vial containing 1.00 mL of a 50:50 v/v DMeF and DMeTHF mixture. The relative uptake amount of MeF or DMeF in HB3 α was measured by heating the crystals to release the adsorbed vapor

using GC method. Before measurement, the crystals were heated at 60 °C to remove the surface-physically adsorbed vapor.

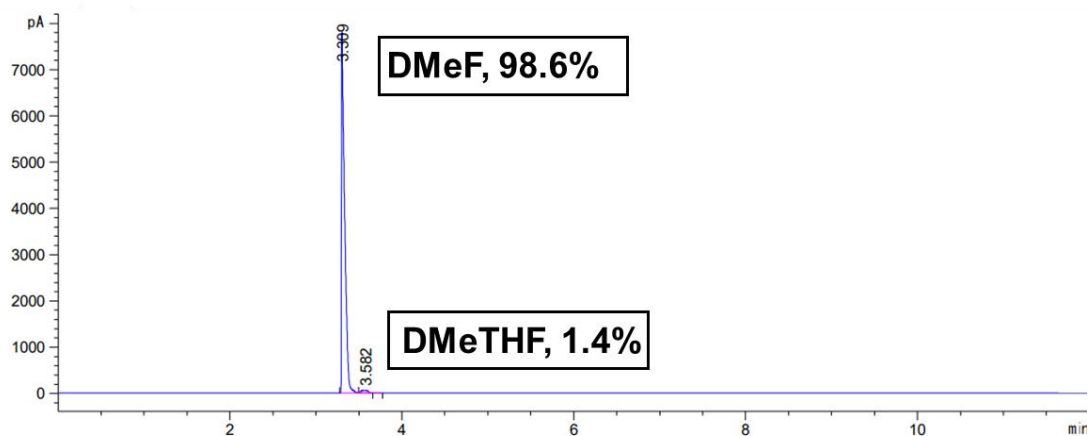


Fig. S20. GC measurements of the relative uptake of **DMeF/DMeTHF** in **HB3 α** after 20.00 mg of crystals were put in 1 mL of a 50:50 v/v **DMeF/DMeTHF** mixture for 30 hours.

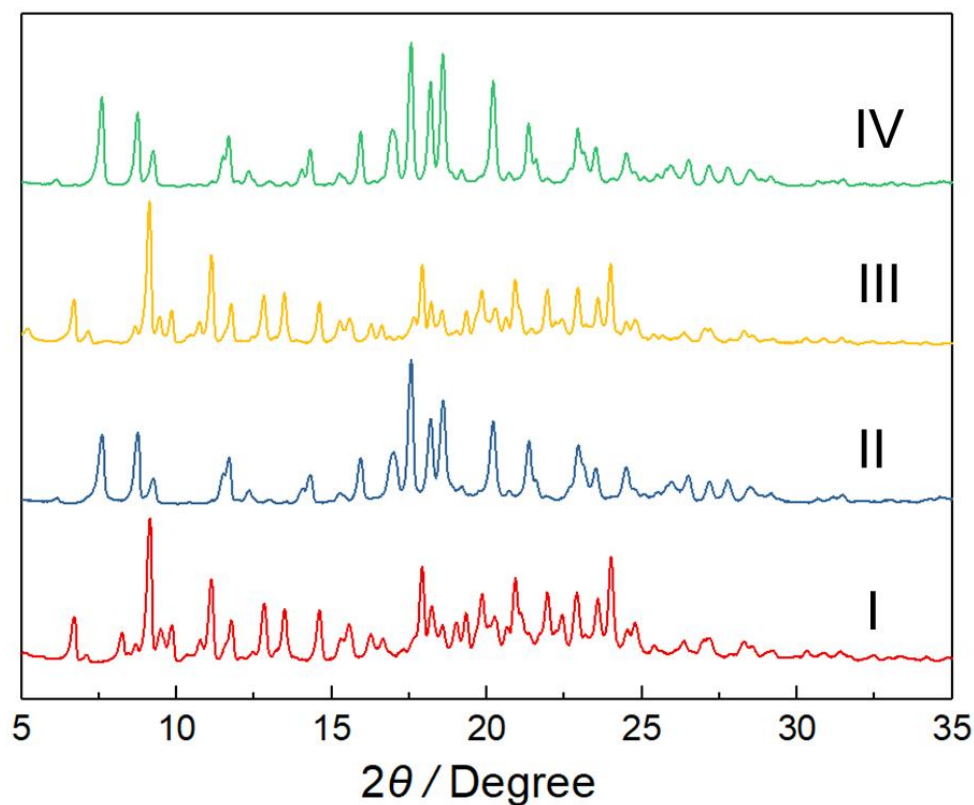


Fig. S21. PXRD patterns of **HB3**: (I) activated **HB3 α** ; (II) after adsorption of **DMeF** vapor; (III) after adsorption of **DMeTHF** vapor; (IV) after adsorption of a 50:50 v/v **DMeF** and **DMeTHF** mixture vapor.

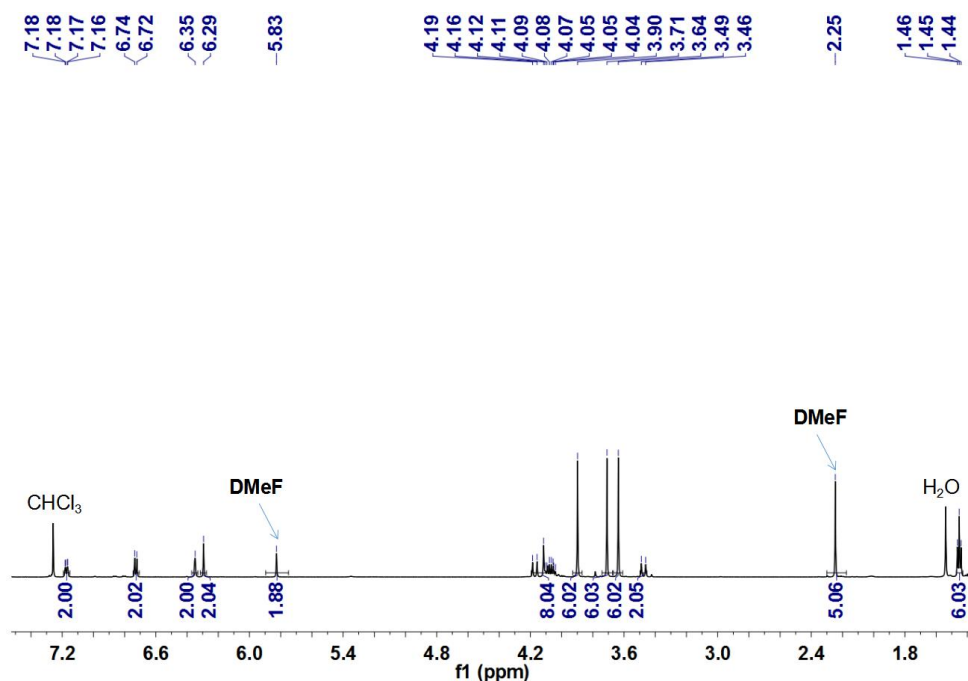


Fig. S22. ^1H NMR spectrum (600 MHz, chloroform-*d*, 298 K) of **HB3 α** after adsorption of a 50:50 v/v **MeF** and **DMeTHF** mixture vapor.

5. Recycling Experiments of Hybrid[3]arene

An open 5.00 mL vial containing 20.00 mg of **DMeF@HB3** was desolvated under vacuum at 150 °C overnight. The resultant crystals were characterized by TGA, PXRD and ^1H NMR methods.

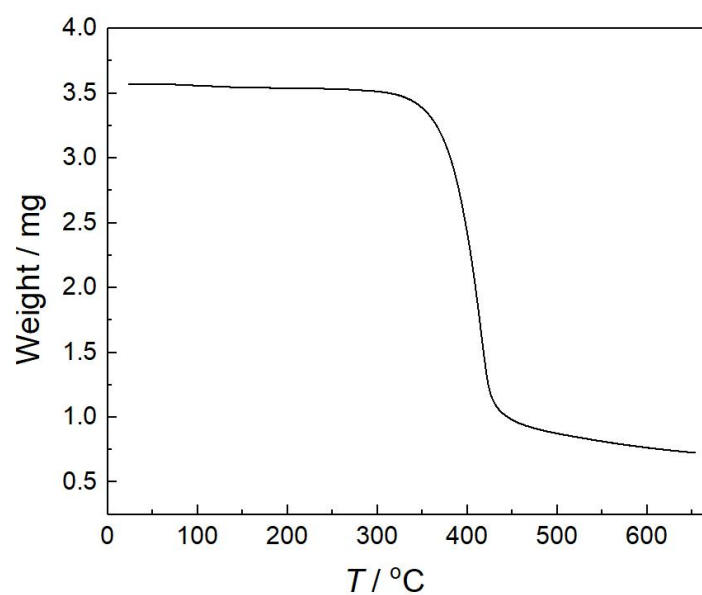


Fig. S23. TGA curve of **DMeF@HB3** after removal of **DMeF**.

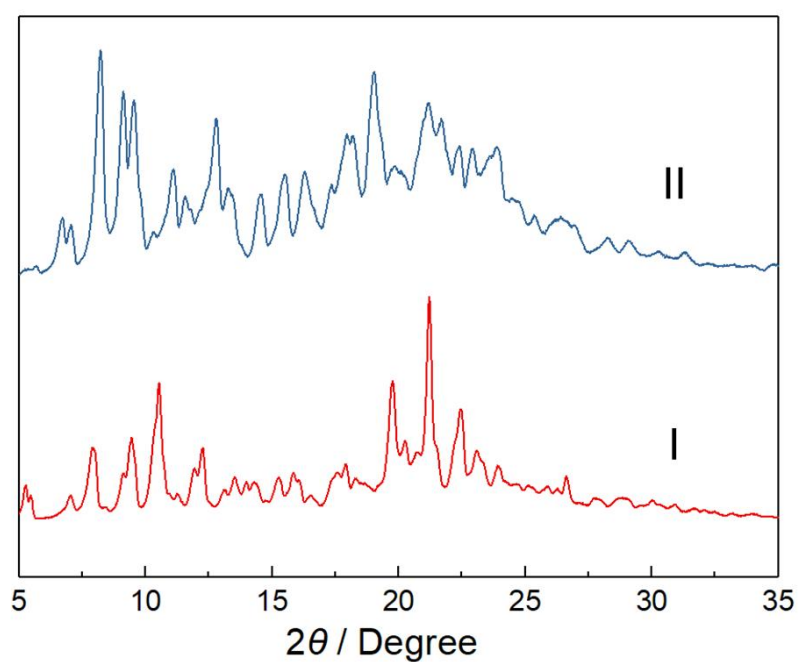


Fig. S24. PXRD patterns of **HB3**: (I) **HB3 α** ; (II) desolvated **DMeF@HB3**. This result indicated that **DMeF@HB3** could transform back to activated **HB3 α** after removal of **DMeF**.

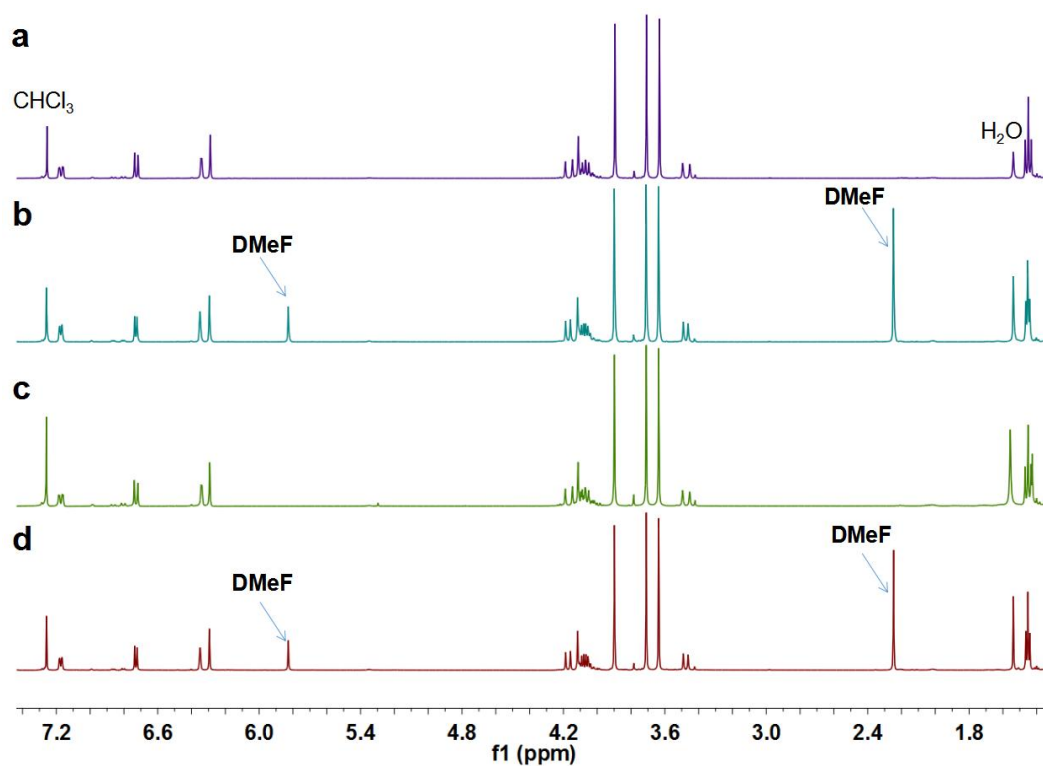


Fig. S25. ^1H NMR spectra (400 MHz, chloroform-*d*, 298 K): (a) original **HB3 α** ; (b) **HB3 α** after adsorption of **DMeF** vapor; (c) **DMeF@HB3** after removal of **DMeF**; (d) desolvated **DMeF@HB3** after adsorption of **DMeF** vapor.

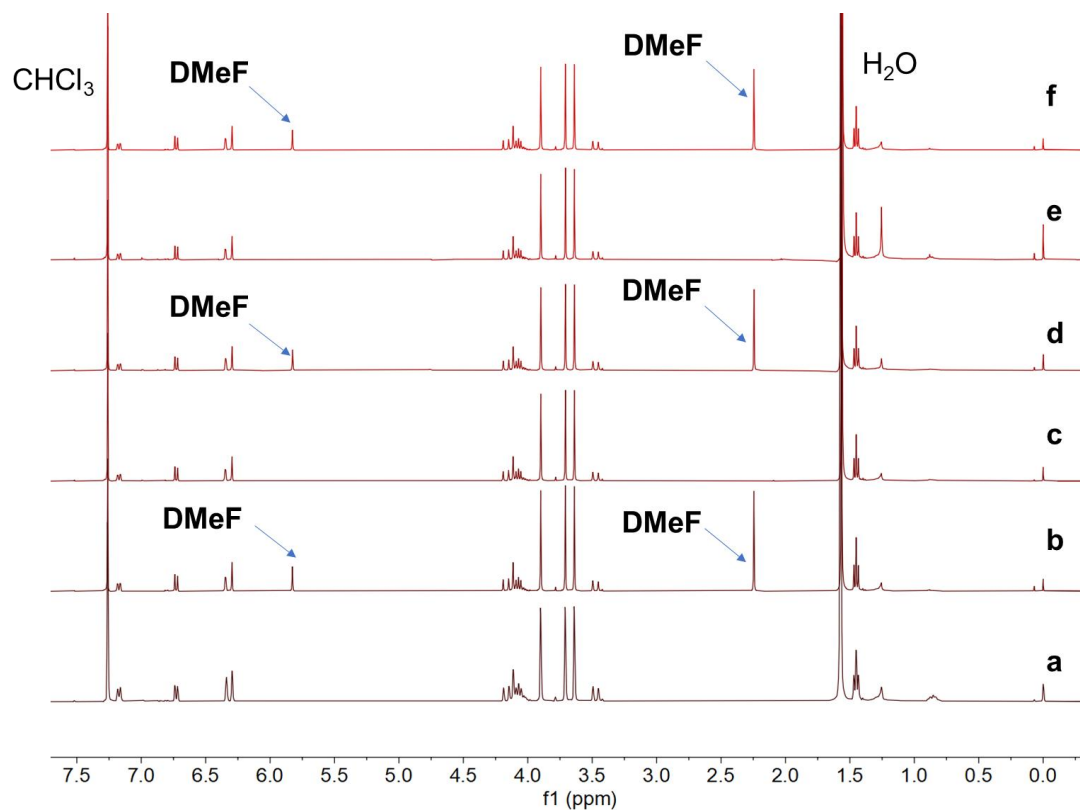


Fig. S26. ^1H NMR spectra (400 MHz, chloroform-*d*, 298 K): (a) original **HB3 α** ; (b) **HB3 α** after adsorption of **DMeF** vapor; (c) **DMeF@HB3** after removal of **DMeF** with five cycles; (d) desolvated **DMeF@HB3** after adsorption of **DMeF** vapor with five cycles; (e) **DMeF@HB3** after removal of **DMeF** with ten cycles; (f) desolvated **DMeF@HB3** after adsorption of **DMeF** vapor with ten cycles.

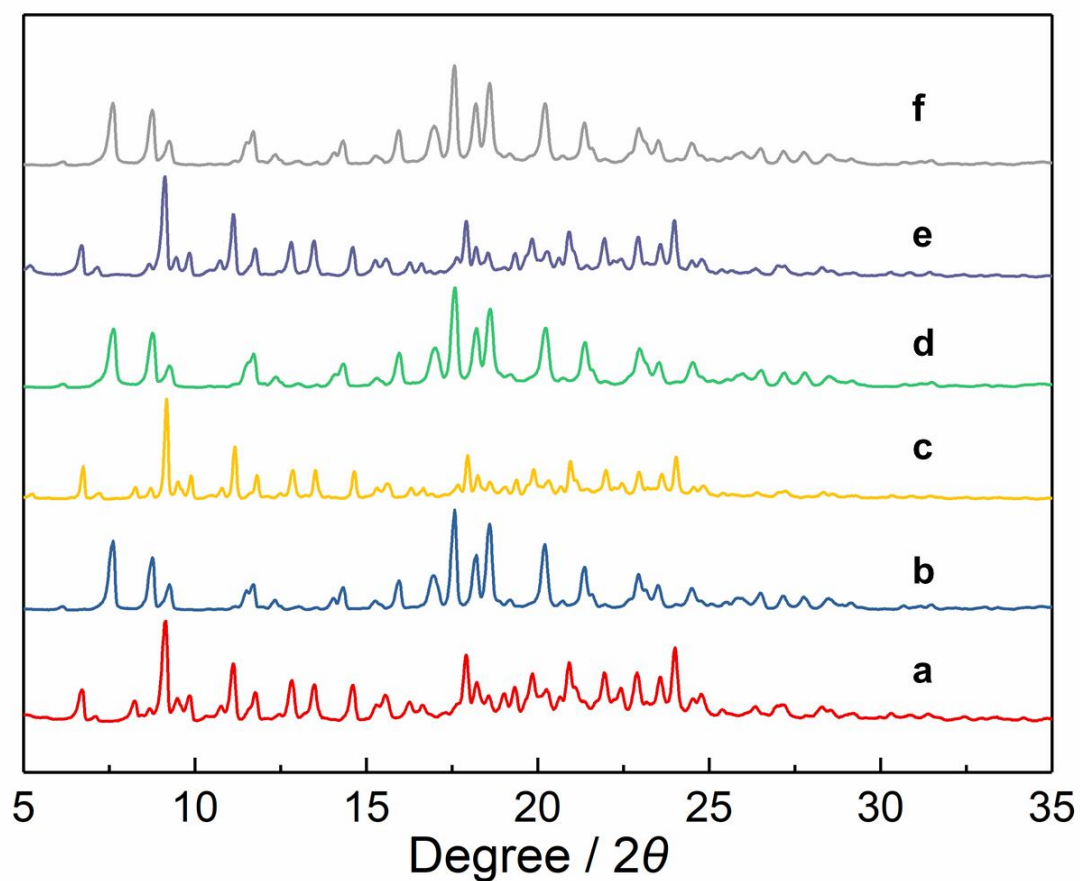


Fig. S27. PXRD patterns of **HB3**: (a) original **HB3 α** ; (b) **HB3 α** after adsorption of **DMeF** vapor; (c) **DMeF@HB3** after removal of **DMeF** with five cycles; (d) desolvated **DMeF@HB3** after adsorption of **DMeF** vapor with five cycles; (e) **DMeF@HB3** after removal of **DMeF** with ten cycles; (f) desolvated **DMeF@HB3** after adsorption of **DMeF** vapor with ten cycles.

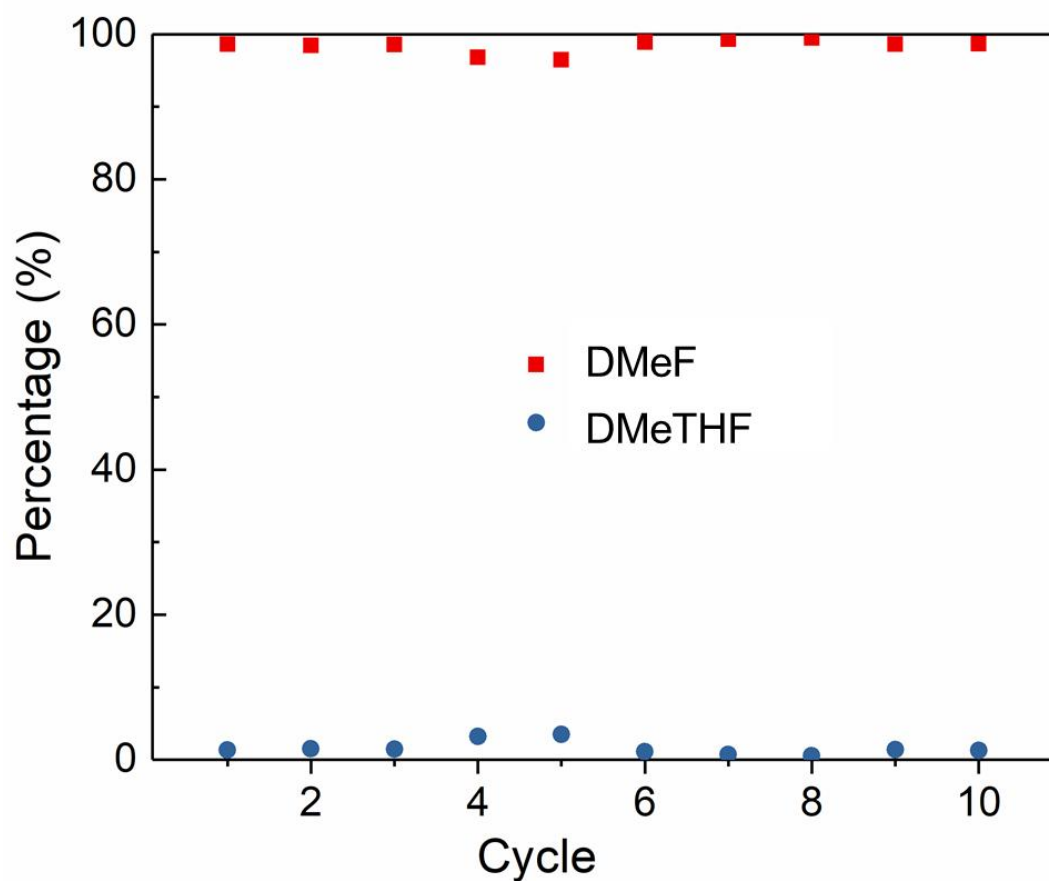


Fig. S28. Relative uptake of **DMeF** and **DMeTHF** by **HB3 α** over 30 hours after **HB3 α** was recycled ten times.

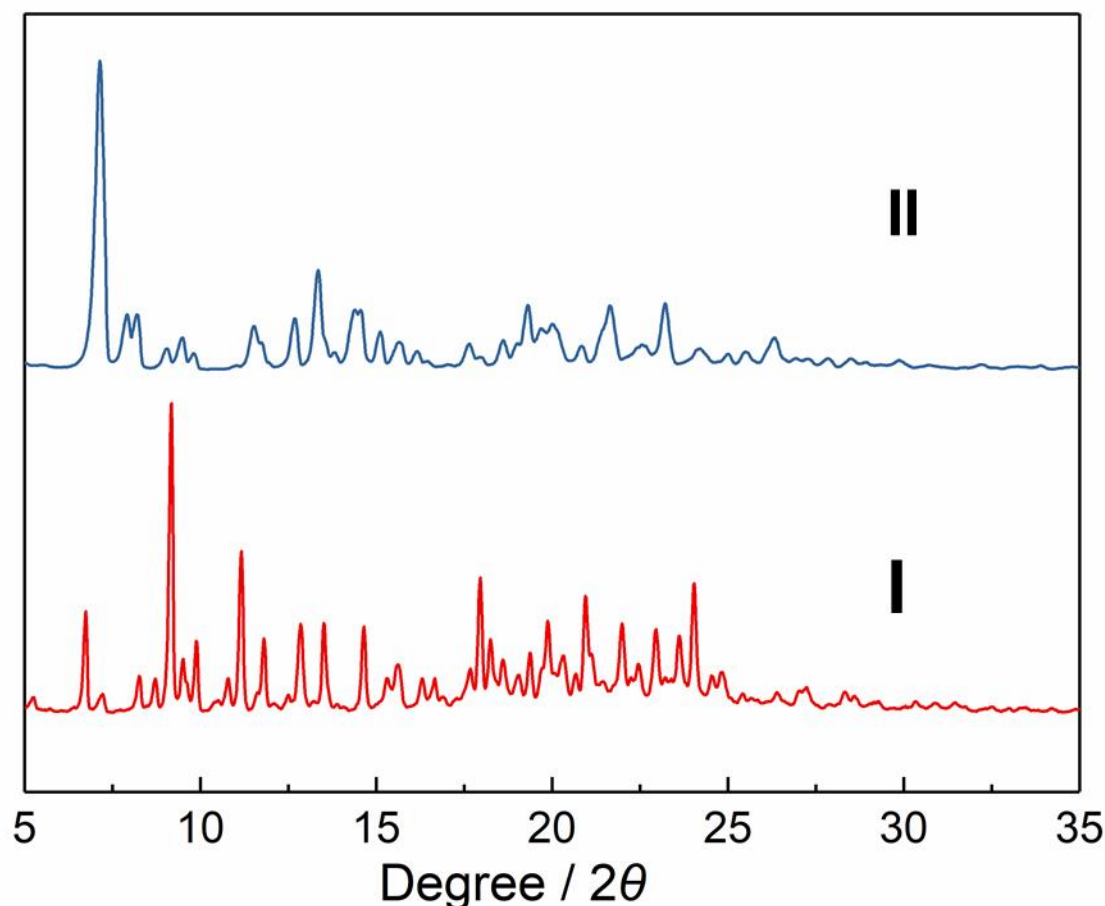


Fig. S29. PXRD patterns of **HB3**: (I) activated **HB3**; (II) initial synthetic **HB3**.

6. References

- [S1] J. Zhou, J. Yang, B. Hua, L. Shao, G. Yu, *Chem. Commun.* **2016**, 52, 1622–1624.
- [S2] K. Jie, M. Liu, Y. Zhou, M. A. Little, A. Pulido, S.-Y. Chong, A. Stephenson, A. R. Hughes, F. Sakakibara, T. Ogoshi, F. Blanc, G. M. Day, F. Huang, A. I. Cooper, *J. Am. Chem. Soc.* **2018**, *140*, 6921–6930.
- [S3] D. R. Lide, *CRC Handbook of Chemistry and Physics*, Boca Raton, FL, **2005**, pp. 203–365.
- [S4] Gaussian 09, Revision A.02; M. J. Frisch, G. W. Trucks, H. B. Schlegel, G. E. Scuseria, M. A. Robb, J. R. Cheeseman, G. Scalmani, V. Barone, B. Mennucci, G. A. Petersson, et al. Gaussian, Inc.: Wallingford, CT, **2009**
- [S5] C. Lee, W. Yang, R. Parr, Development of the Colle-Salvetti correlation-energy formula into a functional of the electron density, *Phys. Rev. B.* **1988**, *37*, 785–789.
- [S6] R. Ditchfield, W. Hehre, J. Pople, Self-consistent molecular-orbital methods. IX. An extended gaussian-type basis for molecular-orbital studies of organic molecules, *J.*

Chem. Phys. **1971**, *54*, 724–728.